ELSEVIER

Polymer 41 (2000) 9003–9010

polymer

www.elsevier.nl/locate/polymer

The role of hydrogen bonding in rigid-rod polymers: the crystal structure of a polybenzobisimidazole model compound

D.W. Tomlin[a], A.V. Fratini[b,*], M. Hunsaker[a], W. Wade Adams[a]

[a]*Air Force Research Laboratory, Materials and Manufacturing Technology Directorate, AFRL/ML, Wright Patterson AFB, OH 45433, USA*
[b]*Department of Chemistry, University of Dayton, Dayton, OH 45469-2357, USA*

Dedicated to the memory of Professor Andrew Keller, friend, colleague, and mentor, whose facination with polymer physics he enthusiastically shared wherever he ventured. Andrew's interest in rigid-rod polymers was the catalyst for a professional dialogue that continued for decades, an interaction that we deeply cherish and greatly miss

Received 14 January 2000; received in revised form 13 March 2000; accepted 13 March 2000

Abstract

Microstructural information about the nature of the polymer–water interaction in rigid-rod polybenzimidazole polymer fibers (PBI) is derived from the X-ray crystallographic analysis of 1,7-dihydro-2,6-diphenylbenzo-[1,2-d;4,5-d′]diimidazole tetrahydrate, $C_{20}H_{14}N_4 \cdot 4H_2O$, MW = 382.20 amu, a model compound for poly(*p*-phenylene-benzobisimidazole) (PBDI). The model compound crystallizes in a monoclinic crystal system, space group $P2_1/c$, with $a = 9.008(2)$ Å, $b = 24.967(7)$ Å, $c = 9.870(5)$ Å, $\beta = 119.82(3)°$, and $Z = 4$. Molecules pack in a herringbone fashion, interspersed with a network of solvent water molecules. Hydrogen-bonded water molecules bridge molecules of the model compound that are related by an inversion center. Each water molecule acts both as a hydrogen bond donor and as a hydrogen bond acceptor. A plausible model for the packing of chains in heat-treated fibers of PBDI would involve polymer chains extending in the direction of elongation, in the manner found for polybenzothiazoles (PBZT) and polybenzoxazoles (PBO), but with a network of hydrogen-bonded water molecules providing strong lateral interactions between polymer molecules. A comparison is made with the structure of poly-{2,6-diimidazo[4,5-b:4′,5′-e]pyridinylene-1,4(2,5-dihydroxy) phenylene} (PIPD or 'M5' fiber) since the enhanced compressive behavior of PIPD is attributed to a hydrogen-bonding network between polymer chains. © 2000 Published by Elsevier Science Ltd.

Keywords: Polybenzobisimidazole model compound; Crystal structure; Rigid-rod polymer fibers

1. Introduction

Polymers are useful as structural materials due to their high strength-to-weight ratio, ease of processing, and availability of structural variations to control both mechanical and physical properties. In response to the need for high temperature adhesives and coatings, heat resistant fibers and ablative systems, polymer scientists have long been active in research in the area of thermally stable polymers. Particular emphasis in our laboratory has been placed on the high temperature resistant, rod-like, aromatic heterocyclic polymers shown below. The *p*-configured poly(*p*-phenylenebenzobis-oxazole) (PBO) and poly(*p*-phenylenebenzobisthiazole) (PBZT), in particular, demonstrate high tensile strength, high modulus and good thermooxidative stability when solutions are spun into films and fibers [1–5].

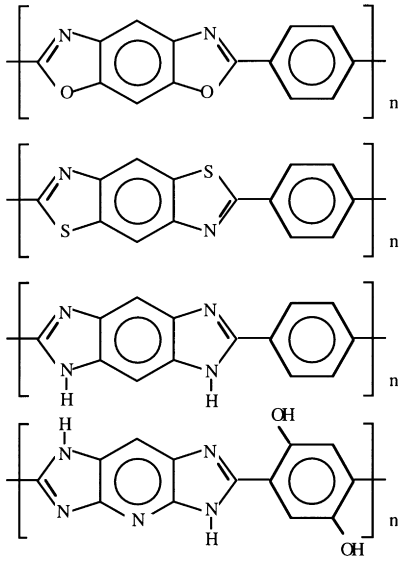

* Corresponding author. Fax: + 1-937-229-2635.
E-mail address: fratini@neelix.udayton.edu (A.V. Fratini).

0032-3861/00/$ - see front matter © 2000 Published by Elsevier Science Ltd.
PII: S0032-3861(00)00242-1

As a class of polymers, the polybenzimidazoles (PBI) are also notable as heat resistant polymers. Thermogravimetric analysis of wholly aromatic PBIs showed weight losses starting around 600°C, reaching about 30% at 900°C [6]. Unfortunately, these PBIs exhibit a high affinity for water, making PBIs less attractive as structural materials when compared to PBO and PBZT. Even after days of drying in a vacuum oven, 5% or more water is retained in the polymer. Similarly, in (*p*-phenylenebenzo-diimidazole) polymer (PBDI), the hydrophilicity is so pronounced that prolonged heating under vacuum does not eliminate the water completely. Unpublished evidence exists for the use of PBDI to dry "Drierite". Recently, the Akzo Nobel Company reported on the synthesis of a modified PBI, namely poly-{2,6-diimidazo[4,5-b:4′,5′-e]pyridinylene-1,4(2,5-dihydroxy) phenylene}, PIPD, (or 'M5' in its fiber form) [7–9]. PIPD contains a diimidazopyridinylene ring system and symmetric –OH substituents on the *p*-phenylene group (Ph group). PIPD fibers exhibit the high stiffness and tenacity of PBO and PBZT, but with a compressive strength that is much higher than other rigid-rod polymers (1.7 GPa) [8,10,11]. The enhanced chain stiffness and superior compressive behavior of heat-treated fibers of PIPD can be attributed to a network of intramolecular and intermolecular hydrogen bonds [9,12].

The problem of thermal stability versus tractability is exemplified in a class of materials known as semi-ladder polymers. These aromatic heterocyclic systems derive their thermal stability from the aromatic nature and stiffness of the chain. The structural characteristics that give these materials their superior thermal and mechanical properties also make them difficult to process [13]. Various molecular composites have been studied for their mechanical and morphological properties as well as their tractability [14]. In several of the initial blends studied, PBDI functioned as the reinforcing component, albeit at a fairly low MW [15].

With PIPD, high MW polymer was achieved from a polyphosphoric acid (PPA) solution containing the tetraaminopyridine (TAP)–dihydroxyterephthalic acid (DHTA) 1:1 complex, abbreviated the TAP.DHTA 1:1 complex or TD-salt [7]. By polymerizing through the TD salt, the rate of polymerization was enhanced significantly and some of the experimental difficulties inherent in the traditional method were avoided [9].

X-ray (XRD) studies on polymers are facilitated by the structure determination of model compounds [16–20]. Detailed structure information on individual polymer blend components can be extrapolated from the molecular geometry of the model compound. For example, interpretation of XRD patterns of PBO and PBZT relied heavily on the crystal structure analysis of the model compounds 2,6-diphenyl-benzo(1,2-d;5,4-d′)-bisoxazole (*cis*-bisoxazole) and 2,6-diphenylbenzo(1,2-d;4,5-d′)-bisthiazole (*trans*-bisthiazole) [16,21]. The fiber patterns of PBZT exhibit strong Bragg equatorial reflections at 3.4 and 5.9 Å, and many meridional layer lines corresponding to a fiber repeat distance of 12.41(3) Å. Based on a comparison to model compound crystal structures, these equatorial spacings have been interpreted as the lateral separation of adjacent polymer chains that are packed as highly oriented rods of high chemical perfection.

This report presents the crystal structure analysis of 1,7-dihydro-2,6-diphenylbenzo-[1,2-d;4,5-d′]diimidazole tetrahydrate, a model compound for PBDI, hereafter referred to as the diimidazole model compound. This structure provides not only accurate molecular parameters for the monomer repeat unit for use in the structural analysis of PBI fibers and blends, but also gives insight into the nature of the polymer–water interaction in PBIs [22].

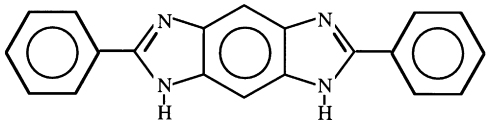

diimidazole model compound

2. Experimental methods

2.1. Synthesis

The diimidazole model compound was prepared by Dr Fred Arnold of AFRL. The synthesis followed the original procedure of Vogel and Marvel [23], in which the stoichiometric combination of tetraamine and phenyl benzoate in melt condensation gave the desired product 1,7-dihydro-2,6-diphenylbenzo-[1,2-d;4,5-d′]diimidazole tetrahydrate ($C_{20}H_{14}N_4 \cdot 4H_2O$, MW = 382.20 amu). Single crystals suitable for crystallographic analysis were obtained by vacuum sublimation at 360°C and by slow evaporation from ethanol.

The ethanol-grown crystals grew as parallelepipeds with an amber tint, whereas sublimation yielded clusters of single crystals similar in morphology to the ethanol-grown crystals though smaller in size. The diffraction characteristics of the ethanol-grown crystals were superior to those of the sublimed crystals. PBIs are known to be hygroscopic. Microscopic inspection of the crystals after standing for several months at room temperature and humidity showed no deterioration, probably because the equilibrium water content had already been achieved during crystal growth.

2.2. DSC

DSC data indicate higher lattice energies for the diimidazole model compound compared to the PBO and PBZT model compounds. Whereas melting endotherms are observed at approximately 300°C for PBO and PBZT model compounds (the T_m of the PBO model compound is obscured by the onset of sublimation), the diimidazole model compound exhibits two broad endotherms at 300

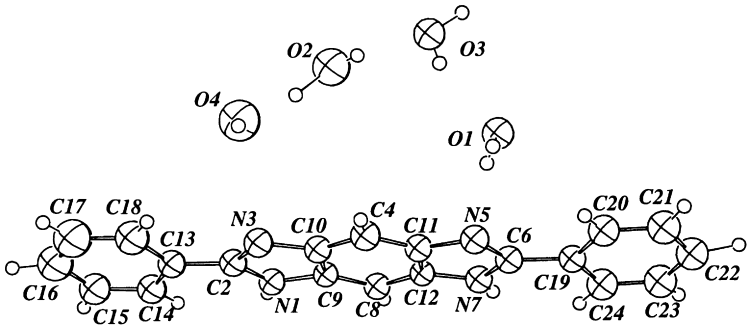

Fig. 1. A thermal ellipsoid plot of the diimidazole model compound, including the numbering scheme.

and 480°C, which are not characteristic of melting transitions but indications of the possible loss of water.

2.3. Density

Crystal densities were measured by flotation in aqueous CsCl. The calculated anhydrous density was 1.07 g/cm^3, based on $Z = 4$. A measured density of 1.295 g/cm^3 for the ethanol-grown crystal was an early indication that the solvent might be incorporated into the structure. This seemed reasonable in light of the characteristic absorption of water by PBI, as mentioned previously. Determination of the structure confirmed the presence of 16 water molecules per unit cell, which raised the calculated density to 1.319 g/cm^3. The sublimed crystals had a similar measured density of 1.304 g/cm^3, suggesting that water was carried along even during sublimation.

Table 1
Fractional coordinates of non-hydrogen atoms, with e.s.d.'s given in parentheses

Atom	x	y	z
O1	0.17974(25)	0.45513(9)	0.66875(23)
O2	0.19769(32)	0.62610(10)	0.83752(29)
O3	0.14868(27)	0.56144(8)	0.58426(24)
O4	0.52865(32)	0.63848(11)	1.07177(31)
N1	0.35231(30)	0.55994(9)	1.43324(27)
C2	0.48124(39)	0.58762(12)	1.43252(35)
N3	0.51130(31)	0.57032(10)	1.32069(29)
C4	0.36788(40)	0.49772(12)	1.11888(37)
N5	0.18440(33)	0.42266(10)	0.94658(28)
C6	0.05893(40)	0.39541(12)	0.94874(35)
N7	0.02811(31)	0.41293(10)	1.06298(28)
C8	0.16171(39)	0.48492(12)	1.26643(36)
C9	0.29073(35)	0.52239(12)	1.31520(32)
C10	0.39337(37)	0.52935(12)	1.24364(34)
C11	0.24056(36)	0.45995(12)	1.06811(33)
C12	0.14001(35)	0.45405(12)	1.14256(33)
C13	0.57338(40)	0.63083(12)	1.54275(36)
C14	0.54190(43)	0.64287(13)	1.66351(39)
C15	0.62653(48)	0.68443(15)	1.76545(42)
C16	0.74292(51)	0.71466(15)	1.74637(45)
C17	0.77927(52)	0.70245(17)	1.62950(49)
C18	0.69150(48)	0.66129(15)	1.52606(42)
C19	−0.04070(39)	0.35251(12)	0.84046(35)
C20	−0.02020(42)	0.34051(13)	0.71344(39)
C21	−0.11988(46)	0.30166(14)	0.60639(40)
C22	−0.23836(45)	0.27288(14)	0.62612(41)
C23	−0.25837(46)	0.28423(15)	0.75261(44)
C24	−0.15977(44)	0.32325(13)	0.86026(39)

2.4. Data collection and structure solution

The ethanol-grown crystal was mounted on the diffractometer with the *a*-axis coincident with ϕ. A total of 11,431 reflections were measured using a θ–2θ scan mode and Nb-filtered MoKα radiation. Intensities were recorded with a scan speed of 1° per minute for reflections of $2\theta < 56°$. The $\mu = 0.877$ cm^{-1} value was calculated using mass absorption coefficients tabulated in the *International Tables, vol. III* [24].

The crystal system is monoclinic, space group $P2_1/c$. Unit cell parameters: $a = 9.008(2)$ Å, $b = 24.967(7)$ Å, $c = 9.870(5)$ Å, $\beta = 119.82(3)°$ and $V = 1925.8(13)$Å^3. The structure was solved by direct methods. Four water molecules were located in difference Fourier maps, which followed several cycles of isotropic full-matrix least-squares refinement. Subsequent difference maps located all 14 hydrogen atoms of the molecule and seven of the eight hydrogen atoms associated with the water structure. A thermal ellipsoid plot of the molecule, including the numbering system, is shown in Fig. 1. The refinement used only $F > 3\sigma$. The structure was refined to a final R value of 0.084 [25]. Fractional coordinates for non-hydrogen atoms are listed in Table 1. Hydrogen atom fractional coordinates are listed in Table 2.

3. Results and discussion

Determination of the structure reveals a slightly non-planar diphenylbenzodiimidazole molecule with semi-localized CN double bonds. The Ph groups are rotated in the same direction from coplanarity with the planar benzodiimidazole moiety by 6.0 and 7.9°, respectively. This twisting of the Ph groups is probably due to crystal packing forces rather than a steric hindrance, as the intramolecular distances between the nitrogen and adjacent *ortho* hydrogen atoms average 2.62 Å, which is close to the normal van der Waals separation of 2.7 Å. The nitrogen atoms with lone electron pairs are positioned *cis* to each other. The monomer

Table 2
Fractional coordinates of hydrogen atoms with e.s.d.'s given in parentheses

Atom	*x*	*y*	*z*
H1	0.3046(30)	0.5647(10)	1.4869(28)
H4	0.4407(30)	0.5009(9)	1.0750(28)
H7	−0.0487(31)	0.4011(9)	1.0794(28)
H8	0.0832(30)	0.4803(10)	1.3042(27)
H14	0.4537(30)	0.6246(9)	1.6705(28)
H15	0.5989(32)	0.6915(10)	1.8529(29)
H16	0.8198(30)	0.7415(11)	1.8291(29)
H17	0.8706(31)	0.7213(10)	1.6221(29)
H18	0.7190(32)	0.6504(10)	1.4459(30)
H20	0.0689(31)	0.3565(10)	0.7043(28)
H21	−0.0995(32)	0.2958(10)	0.5211(30)
H22	−0.3448(30)	0.2474(11)	0.5304(29)
H23	−0.3538(31)	0.2677(10)	0.7611(30)
H24	−0.1707(33)	0.3324(10)	0.9532(29)
HO1	0.3020(35)	0.4414(11)	0.6882(31)
HO2	0.1987(33)	0.4484(10)	0.7515(31)
HO3	0.1739(32)	0.6114(10)	0.7647(30)
HO4	0.3622(30)	0.6234(10)	0.9403(28)
HO5	0.0250(31)	0.5580(10)	0.4921(29)
HO6	0.1727(31)	0.5366(10)	0.6256(28)
HO7	0.5972(34)	0.6274(11)	1.0694(31)

repeat distance, 12.197(6) Å, as measured by the C16–C19 separation, should correspond to the polymer repeat in rod-like polybenzobisimidazoles (PBDI).

Bond lengths and angles with estimated standard deviations are summarized in Tables 3 and 4. Table 5 lists the ring dimensions for several imidazoles taken from the literature. Comparison of the four CN bond lengths obtained in this investigation with values in Table 5 shows that all bonds are within the expected range for a delocalized imidazole system. The imidazole ring geometries in the model compound, however, are slightly asymmetrical about a line passing through the apical carbon, C2 or C6, and bisecting the opposite bond. The difference between the N1–C2 and N3–C2 bond is 0.023 Å (roughly four times the estimated standard deviation); between the N5–C6 and N7–C6 bonds, 0.026 Å. There is also an associated difference of 3.2° between the C2–N3–C10 and C2–N1–C9 bond angles, and of 2.6° between the C6–N5–C11 and C6–N7–C12 bond angles. Though moderate, these differences point to a semi-localization of the CN double bond on the pair with the shorter bond distance, which is consistent with the observation that H1 and H7 are bonded to N1 and N7, respectively. Semi-localization of the CN double bond is characteristic of some benzimidazoles. Selected bond lengths and angles for these benzimidazoles are compared in Table 5.

Table 3
Bond distances (Å) for non-hydrogen atoms with e.s.d.'s given in parentheses

	Distance (Å)		Distance (Å)
N1–C2	1.356(4)	C2–C13	1.468(4)
C2–N3	1.333(5)	C13–C14	1.397(6)
N3–C10	1.399(3)	C14–C15	1.376(4)
C4–C10	1.383(5)	C15–C16	1.374(6)
C4–C11	1.369(4)	C16–C17	1.375(7)
C11–C12	1.428(5)	C17–C18	1.387(5)
N5–C11	1.401(4)	C13–C18	1.378(6)
N5–C6	1.333(4)	C19–C20	1.386(5)
C6–N7	1.359(5)	C20–C21	1.382(4)
N7–C12	1.381(3)	C21–C22	1.375(6)
C8–C12	1.374(4)	C22–C23	1.379(6)
C8–C9	1.376(4)	C23–C24	1.390(4)
C9–C10	1.425(5)	C19–C24	1.385(5)
N1–C9	1.379(3)		

Table 4
Bond angles (°) for non-hydrogen atoms with e.s.d.'s given in parentheses

	Angle (°)		Angle (°)
C2–N1–C9	109.1(3)	N1–C2–C13	123.0(3)
N1–C2–N3	111.6(2)	N3–C2–C13	125.4(3)
C2–N3–C10	105.9(3)	C2–C13–C14	121.1(3)
C4–C10–N3	130.3(3)	C2–C13–C18	120.3(3)
C4–C10–C9	120.7(3)	C13–C14–C15	121.0(4)
N3–C10–C9	109.0(3)	C14–C15–C16	119.7(4)
C10–C4–C11	117.0(4)	C15–C16–C17	120.2(3)
C4–C11–N5	130.5(3)	C16–C17–C18	119.8(4)
N5–C11–C12	108.6(2)	C13–C18–C17	120.6(4)
C4–C11–C12	120.9(3)	C14–C13–C18	118.6(3)
C6–N5–C11	106.0(3)	N5–C6–C19	125.4(3)
N5–C6–N7	111.9(2)	N7–C6–C19	122.7(3)
C6–N7–C12	108.6(3)	C6–C19–C20	120.8(3)
N7–C12–C8	131.7(3)	C6–C19–C24	121.0(3)
N7–C12–C11	104.9(3)	C19–C20–C21	121.2(4)
C8–C12–C11	123.5(3)	C20–C21–C22	120.5(4)
C9–C8–C12	114.5(3)	C21–C22–C23	118.8(3)
N1–C9–C8	132.1(3)	C22–C23–C24	121.0(4)
C8–C9–C10	123.4(3)	C20–C19–C24	118.2(3)
N1–C9–C10	104.5(2)	C19–C24–C23	120.3(4)

Table 5 also lists benzimidazoles in which π-electron density is delocalized over the imidazole ring, as is apparently the case with 2-mercaptobenzimidazole. The crystal structure determination of 2-mercaptobenzimidazole shows hydrogen atoms covalently bonded to both nitrogen atoms, equivalent CN bond lengths which are intermediate between single and double bonds, and a CS double bond [29]. 2-Thio-1-(β-D-ribo-furanosyl)-3-H-benzimidazole is similar to mercaptobenzimidazole in that the apical carbon atom is double bonded to a sulfur atom [30]. Though the imidazole ring is still delocalized, one CN bond is slightly shorter than the other. There is an 0.033 Å difference between the C2–N1 and C2–N3 bond lengths. In contrast, the chloro analog of 2-thio-1-(β-D-ribofuranosyl) benzimidazole shows semi-localization of the CN double bond, with a 0.074 Å difference between the C2–N1 and C2–N3 bond lengths [31].

Benzimidazole has a tendency to form intermolecular hydrogen bonds. The involvement of the electron lone pair on nitrogen in hydrogen bonding lessens its contribution to the π-system in the ring. This would explain in part the apparent semi-localization of electron density on the C2–N1 bond in benzimidazole [32]. The difference in CN

Table 5
Selected ring dimensions of imidazoles and benzimidazoles

Compound	N1–C2 (Å)	C2–N3 (Å)	N3–C4 (Å)	C4–C9 (Å)	C9–N1 (Å)	C–N1–C (°)	C–N3–C (°)	References
Imidazole at −150°C	1.326	1.349	1.369	1.358	1.378			[26]
Imidazole at 24°C	1.311	1.337	1.372	1.311	1.381			[27]
1,3-Dimethylimidazole-2-thione	1.346	1.346	1.390	1.329	1.390			[28]
2-Mercaptobenzimidazole	1.362	1.362	1.383	1.400	1.383	110.4	110.4	[29]
2-Thio-1-(β-D-ribofuranosyl)-3-H-benzimidazole	1.344	1.377				110.9	109.4	[30]
2-Cl-(β-D-ribofuranosyl)benzimidazole	1.293	1.367				104.4	104.1	[31]
Benzimidazole	1.311	1.346				106.6	104.2	[32]
Benzimidazole–benzimidazolium fluoroborate (protonated)	1.320	1.338				109.1	109.8	[33]
Benzimidazole–benzimidazolium fluoroborate	1.306	1.364				105.5	106.9	[33]
Imidazole 5,5-diethyl barbituric acid complex	1.300	1.324				105.2	107.0	[34]
1,3-Dimethyl-2-methylaminobenzimidazolium perchlorate	1.346	1.353	1.396	1.407	1.364	107.2	108.2	[35]
1,3-Dimethyl-2-aminobenzimidazolium perchlorate	1.339	1.349	1.380	1.365	1.405	108.2	109.1	[35]
1,3-Dimethyl-2-dimethylaminobenzimidazolium perchlorate	1.329	1.343	1.380	1.375	1.384	108.8	109.5	[35]
1-Methyl-2-methylaminobenzimidazolium perchlorate	1.368	1.365	1.391	1.364	1.407	110.2	110.4	[35]
Imidazo–benzimidazole complex	1.290	1.382	1.407	1.405	1.405	103.3	106.1	[36]
2-Hydroxymethylbenzimidazole I	1.316	1.359	1.379	1.398	1.388	105.1	107.3	[37]
2-Hydroxymethylbenzimidazole II	1.309	1.353	1.370	1.400	1.396	105.0	107.3	[37]
2,5-Dichloro-1-(*p*-chlorobenzyl)-1H-benzimidazole	1.296	1.361	1.383	1.400	1.391	103.0	104.9	[38]
1-Benzyl-2-(2,6-dichloroanilinomethyl)-1H-benzimidazole	1.308	1.364				104.5	106.1	[39]
2-(3-Methoxy-2-hydroxyphenyl)benzimidazole	1.325	1.371	1.376		1.391	106.1	107.6	[40]
(*E*,*Z*)-2-(2-Chloro-5-nitrostyryl)-1-(1-propenyl)benzimidazole	1.317	1.383	1.387		1.384	105.0	106.0	[41]
2,6-Diphenyl(1,2-d;5,4-d′)benzodiimidazole	1.356	1.333	1.399	1.425	1.379	109.2	106.0	This work

bond lengths is 0.035 Å. An interesting example of the effect of environment on the delocalization of the imidazole ring is found in the benzimidazole–benzimidazolium fluoroborate salt [33], in which the fluoroborate anion forms a salt with one benzimidazole cation. The protonated form has hydrogen atoms covalently bonded to each nitrogen, delocalizing the ring and minimizing differences in bond lengths (0.018 Å).

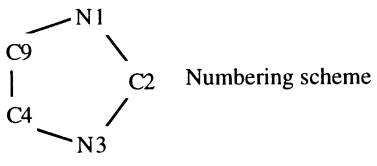

Scheme 1.

The extent of semi-localization in the diimidazole model compound can be qualitatively evaluated in terms of the correlation between the extent of semi-localization and the difference in CN bond lengths. One concludes that the imidazole ring in the model compound exhibits only a slight degree of semi-localization of the CN double bond because of extensive hydrogen bonding of all four nitrogen

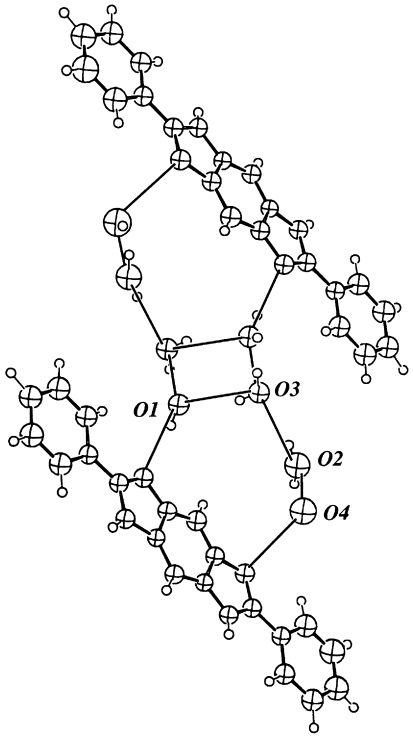

Fig. 2. Water structure bridging a pair of molecules of the diimidazole model compound related by an inversion center. Viewed approximately down the *c*-axis.

atoms with solvent water molecules. This is similar to that observed for 5,5-diethylbarbituric acid–imidazole complex, which experiences hydrogen bonding between N–H···N on the imidazole [34]. The bond length difference between C2–N1 and C2–N3 is slight at 0.024 Å. Bond length differences alone should not be used to determine whether a system is semi-localized or not. Such factors as the contributions to resonance, environment of the molecule, and opportunity for hydrogen bonding must be taken into account.

3.1. Water structure

Elucidation of the water network gives a possible explanation for the preferential crystallization of the *cis* isomer over the *trans* isomer. In all probability, the non-stereospecific synthesis could have resulted in a crystalline product containing both isomers, which in turn would have lead to a disordered crystal structure. However, the hydrogen-bonded network of the *cis* isomer provides a crystalline structure that is more efficiently packed and hence favored over a possible structure involving the *trans* isomer. Additionally, the preference of water for the *cis* isomer could affect the solubility of both isomers, resulting in an unexpected separation of the two isomers during purification and recrystallization of the crude product.

Solvent water molecules form hydrogen bonds bridging molecules related by an inversion center (Figs. 2 and 3). Surprisingly, hydrogen bonding between molecules related by a glide plane is not observed. The network of hydrogen bonding makes maximum use of the four coordination sites on each water molecule. At least three sites are engaged on each water molecule; in the case of O1 and O3, all four coordination sites are occupied. Each water molecule acts both as a hydrogen bond donor and as a hydrogen bond acceptor. The distances range from 2.734 to 3.084 Å, within the expected range for hydrogen bonds. Four water molecules in the asymmetric unit link N3 and N5 to form a large ring (Fig. 1). The ring bends over the molecule, with the best plane containing atoms N3–O4–O1–N5 inclined 37° to the benzodiimidazole plane. The best plane through O4–O2–O3–O1 makes roughly a 53° angle with the N3–O4–O1–N5 plane.

3.2. Crystal packing and polymer fiber structure

The *c*-glide plane perpendicular to the *b*-axis generates two vertical columns of molecules of different orientation, characteristic of a herringbone pattern. The perpendicular distance between adjacent molecules in a stack is 3.93 Å.

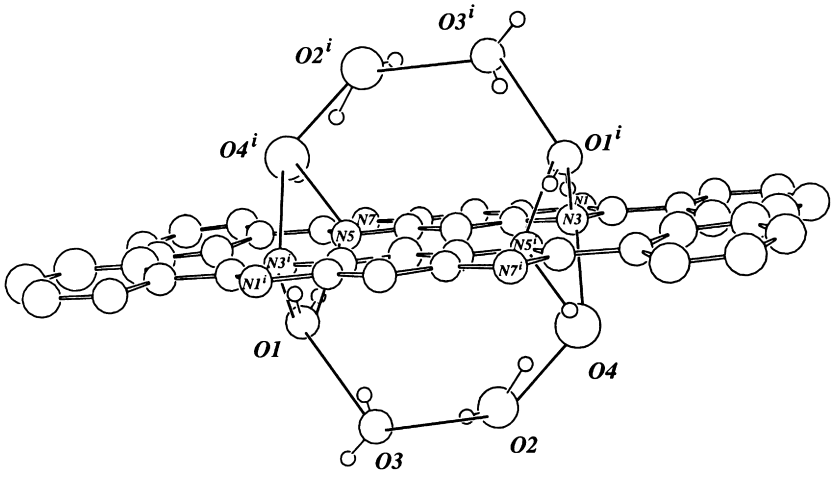

Fig. 3. Water structure bridging a pair of molecules of the diimidazole model compound related by an inversion center. Viewed approximately down the *a*-axis.

The molecules are inclined at an angle of 48.2° to the *b*-axis. Molecules related by a center of symmetry are interspersed with a network of solvent water molecules. Thus, molecules related by an inversion center are intricately connected through hydrogen bonds, while weaker van der Waals interactions connect molecules related by the glide plane. Delocalization of the fused ring system accounts for the high degree of planarity in the *cis*-bisoxazole model compound. Planarity in *trans*-bisthiazole is precluded by the steric clash between nitrogen and sulfur atoms on the thiazole ring with *ortho* hydrogen atoms on the Ph groups, resulting in a torsion angle of 23.2° between the benzobisthiazole moiety and the Ph groups [16]. In the fiber structure of PBO, we reported a torsion angle of 13.0° [21]. Recent neutron diffraction studies on PBO report a torsion angle of 25.7 ± 5.8° at 295 K [42]. No hydrogen bonding occurs in *cis*-bisoxazole and *trans*-bisthiazole; thus, packing forces are of the van der Waals type. The low heat of sublimation in *cis*-bisoxazole reflects the absence of significant intermolecular interaction in the crystal.

In the case of PIPD, a hydrogen-bonding scheme has been proposed involving intermolecular N–H···O hydrogen bonds and intramolecular O–H···N hydrogen bonds [9,12]. The intermolecular hydrogen bonds comprise a bidirectional network of hydrogen bonds linking each polymer chain to its four axially shifted neighboring chains. The enhanced compressive behavior of heat-treated fibers of PIPD is also attributed to this hydrogen-bonding network. A torsion angle of 8.1° between the dihydroxyphenylene and diimidazopyridinylene moieties was calculated using an energy minimization procedure [9].

This work makes possible certain predictions concerning the fiber structure of PBDI and PBI polymer in general. (a) Fibers or films spun from concentrated dopes of high MW PBDI in PPA solvent should be highly oriented and exhibit three-dimensional crystallinity. For high MW PBDI, nonstereo-specific synthesis could produce an irregular structure, thus making it difficult to show three-dimensional crystallinity. These materials would be expected to have an axial tensile modulus comparable to PBZT, but with higher tensile strength and significantly higher lateral strength and compressive strength/modulus due to the formation of a hydrogen-bonded water network laterally linking polymer chains. In the absence of any fiber diffraction data for PBDI, a plausible model for the packing in oriented fibers would involve polymer chains extending in the direction of elongation, in the manner found for PBZT [17,18]. A hydrogen-bonded water structure, which plays an important role in the crystal packing of the model compound, would then provide strong lateral interactions between polymer chains. Given the increased lattice strength due to these intermolecular forces, it is expected that PBDI would have a higher T_m and enhanced compressive strength than either PBO or PBZT, as these polymer molecules would be held in a crystalline lattice solely by van der Waals forces. (b) PBDI bulk material should have a significant energy absorption mechanism due to the hydrogen-bonded water molecules. For example, an infrared or ultraviolet laser beam would have to deposit much more energy to damage this polymer backbone than for PBZT or PBO, since the loss of water would itself dissipate a great deal of absorbed energy. (c) The problem of water retention in PBIs would be partially eliminated by the placement of appropriate substituents on the imidazole nitrogen atoms. This would allow PBI to be used as a structural material without the dimensional changes caused by the binding of water. These conclusions are reinforced by the success of Akzo Nobel Company in preparing high MW polypyridobisimidazole polymer (PIPD).

4. Conclusions

The crystal structure analysis of the diimidazole model compound has provided molecular structure information applicable to polymeric benzimidazoles, and in particular, to rod-like benzimidazoles. The structure determination is useful both for homopolymer structural studies and for morphological investigations of blends and molecular composites.

One can begin to understand why it was not possible to synthesize high MW, rod-like benzimidazole polymers, and specifically PBDI. At low MW, oligomers probably crystallize out of polyphosphoric acid (PPA) solution before the condensation polymerization is very far advanced, due to preferential formation of a stable hydrogen-bonded network in the presence of the excess water of condensation. This hydrogen-bonded structure is apparently more energetically favorable than the fully protonated molecular species dissolved in the solvent. In contrast, PIPD attains high MW via the formation of the TAP.DHTA (1:1) complex, the TD salt, which affords a fast polymerization cycle (4–5 h rather than 24 h or more as reported for rod-like polymers). This synthetic procedure has the advantage of eliminating low MW polymer that results when amine is polymerized with acid in PPA medium.

It is also clear why PBO and PBZT are not water sensitive. The benzimidazoles have two types of nitrogen atoms, one that is protonated and one that possesses the lone electron pair. In order to form a stable water network both types are necessary, one functioning as a proton donor and the other as a proton acceptor. PBOs and PBZTs have only lone pair electron nitrogen atoms, and in addition, the increased delocalization present in the heterocyclic rings may contribute to the lack of hydrogen bonding to water. The variation in the strength of the hydrogen bonds in PBIs probably results in the reversibility of water uptake, since some of the bonds can be broken more easily than others.

Acknowledgements

A preliminary account of this work was presented in

Marilyn Hunsaker's MS thesis submitted to the Chemistry Department at Wright State University.

References

[1] Allen S, Farris R. MRS Symp Proc 1989;134:297–306.
[2] Im J, Percha P, Yeakle D. MRS Symp Proc 1989;134:307–12.
[3] Jiang H, Eby R, Adams WW, Lenhert PG. MRS Symp Proc 1989;134:341–50.
[4] Tashiro K, Yoshino J, Kitagawa T, Murase H, Yabuki K. Macromolecules 1998;31:5430–40.
[5] Kitagawa T, Murase H, Yabuki K. J Polym Sci, Part B: Polym Phys 1998;36:39–48.
[6] Frazer AH. Polym Rev 1968;17:138–213.
[7] Sikkema DJ. Polymer 1998;39:5981–6.
[8] Lammers M, Klop EA, Northolt MG, Sikkema D. Polymer 1998;39:5999–6005.
[9] Klop EA, Lammers M. Polymer 1998;39:5987–98.
[10] van der Jagt OC, Beukers A. Polymer 1999;40:1035–44.
[11] Sirichaisit J, Young RJ. Polymer 1999;40:3421–31.
[12] Hageman JCL, van der Horst JW, de Groot RA. Polymer 1999;40:1313–23.
[13] Husman P, Helminiak T, Adams W. Resins for aerospace. ACS Symp Ser 1980;132:203–14.
[14] Krause SJ. MRS Symp Proc 1989;134:511–22.
[15] Hwang W, Wiff D, Benner C, Helminiak T. J Macromol Sci, Phys Edn B 1983;22:231–57.
[16] Wellman M, Adams W, Wolff R, Dudis D, Wiff D, Fratini A. Macromolecules 1981;14:935–9.
[17] Adams W, Azaroff L, Kulshreshtha A. Z Kristallogr 1979;150:321–6.
[18] Roche E, Takahashi T, Thomas T. Fiber diffraction methods. ACS Symp Ser 1980;141:303–13.
[19] Odell J, Keller A, Atkins E, Miles M. J Mater Sci 1981;16:3309–18.
[20] Wellman M, Adams W, Wiff D, Fratini A. Report AFML-TR-79-4184, Part I, 1980.
[21] Fratini AV, Lenhert PG, Resch TJ, Adams WW. MRS Symp Proc 1989;134:431–45.
[22] Hunsaker M, Adams W, Fratini A. Report AFWAL-TR-83-4055, 1983.
[23] Vogel H, Marvel C. J Polym Sci 1961;50:511–39.
[24] The International Tables for X-ray Crystallography, vol. III. Birmingham, UK: Kynoch Press, 1962.
[25] Stewart J, Kruger G, Ammon H, Dickinson C, Hall S. TR-192: the X-ray System of Crystallographic Programs 1972. University of Maryland Computer Center.
[26] Martinez-Carrera S. Acta Crystallogr 1966;22:91–3.
[27] Will G. Z. Kristallogr 1969;129:211–21.
[28] Tomlin DW, Campbell DP, Fleitz PA, Adams WW. Acta Crystallogr C 1997;53:1153–4.
[29] Form G, Raper E. Acta Crystallogr B 1976;32:345–8.
[30] Prusiner P, Sundaralingam M. Acta Crystallogr B 1973;29:2328–34.
[31] Sprang S, Sundaralingam M. Acta Crystallogr B 1973;29:1910–6.
[32] Dik-Edixhouven C, Schenk H, van der Meer H. Crystal Struct Commun 1973;2:23–4.
[33] Quick A, Williams D. Can J Chem 1976;54:2482–7.
[34] Hsu I, Craven B. Acta Crystallogr B 1974;30:988–93.
[35] Benassi R, Grandi R, Pagnoni U, Taddei F, Bocelli G, Sgarabotto P. J Chem Soc, Perkin Trans 2 1985;10:1513–21.
[36] Molina P, Alajarin M, Lopez-Leonardo C, Madrid I, Foces-Foces C, Cano F. Tetrahedron 1989;45:1823–32.
[37] Aubry A. Acta Crystallogr C 1995;51:115–6.
[38] Kendi E, Ozbey S, Goker H. Acta Crystallogr C 1999;55:243–5.
[39] Kendi E, Ozbey S, Tuncbilek M, Goker H. Acta Crystallogr C 1998;54:854–6.
[40] Elerman Y, Kabuk M. Acta Crystallogr C 1997;53:372–4.
[41] Bacelo D, Cox O, Rivera L, Cordero M, Huang S. Acta Crystallogr C 1997;53:907–9.
[42] Takahashi Y. Macromolecules 1999;32:4010–4.